Cell Reports

The Zebrafish Dorsolateral Habenula Is Required for Updating Learned Behaviors

Graphical Abstract

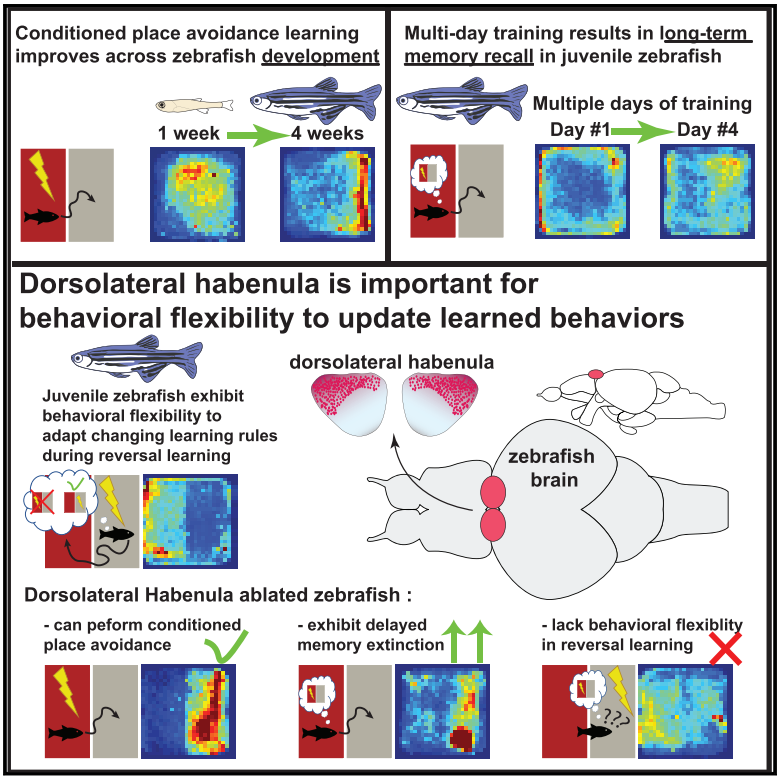

Highlights

- Conditioned place avoidance (CPA) learning improves across zebrafish development
- Juvenile zebrafish form long-term memories after multiple days of CPA training
- Ablation of the dorsolateral habenula (dlHb) delays memory extinction
- dlHb is important for behavioral flexibility to update learned behaviors

Authors

Fabrizio Palumbo, Bram Serneels, Robbrecht Pelgrims, Emre Yaksi

Correspondence

emre.yaksi@ntnu.no

In Brief

Palumbo et al. show that juvenile zebrafish can perform conditioned place avoidance (CPA) learning with improved performance across development and repeated training sessions. The authors demonstrate a role for dorsolateral habenula in providing behavioral flexibility, allowing animals to adapt to changing rules during reversal learning.

Palumbo et al., 2020, Cell Reports *32*, 108054
August 25, 2020
https://doi.org/10.1016/j.celrep.2020.108054

Cell Reports

CellPress
OPEN ACCESS

Report

The Zebrafish Dorsolateral Habenula Is Required for Updating Learned Behaviors

Fabrizio Palumbo,[1] Bram Serneels,[1,2] Robbrecht Pelgrims,[1] and Emre Yaksi[1,3,*]
[1]Kavli Institute for Systems Neuroscience and Centre for Neural Computation, Faculty of Medicine and Health Sciences, Norwegian University of Science and Technology, 7030 Trondheim, Norway
[2]KU Leuven, 3000 Leuven, Belgium
[3]Lead Contact
*Correspondence: emre.yaksi@ntnu.no
https://doi.org/10.1016/j.celrep.2020.108054

SUMMARY

Operant learning requires multiple cognitive processes, such as learning, prediction of potential outcomes, and decision-making. It is less clear how interactions of these processes lead to the behavioral adaptations that allow animals to cope with a changing environment. We show that juvenile zebrafish can perform conditioned place avoidance learning, with improving performance across development. Ablation of the dorsolateral habenula (dlHb), a brain region involved in associative learning and prediction of outcomes, leads to an unexpected improvement in performance and delayed memory extinction. Interestingly, the control animals exhibit rapid adaptation to a changing learning rule, whereas dlHb-ablated animals fail to adapt. Altogether, our results show that the dlHb plays a central role in switching animals' strategies while integrating new evidence with prior experience.

INTRODUCTION

The ability to predict threats or rewards and to shape behavior in response to a changing environment is essential for survival (Skinner, 1984). Operant learning requires a continuous monitoring of the animal's own actions, a real-time estimation of its consequences, and an update of the relationship between the behavior and its outcome (Skinner, 1981). The constant update of this relationship is essential because, in real life, rules and conditions frequently change. Therefore, a high degree of behavioral flexibility is required to maximize survival chances. Reversal learning has been extensively used to evaluate behavioral flexibility (Izquierdo et al., 2017; Hadar and Menzel, 2010). Not surprisingly, the impairment of this behavioral flexibility leads to neuropsychiatric conditions (Baker et al., 2015), such as obsessive-compulsive behaviors (Remijnse et al., 2009), substance abuse (Bechard et al., 2018), post-traumatic stress (George et al., 2015), and mood disorders (Remijnse et al., 2009). Understanding the neural basis of operant learning and the associated behavioral flexibility is essential to provide solutions to these disorders.

The habenula (Hb) plays an important role in operant learning. Mammalian lateral Hb (lHb) receives inputs from various forebrain and midbrain regions and project to the ventral tegmental area (VTA) and raphe nuclei (Bianco and Wilson, 2009; Namboodiri et al., 2016; Fore et al., 2018; Stamatakis and Stuber, 2012; Matsumoto and Hikosaka, 2007, 2009; Lazaridis et al., 2019; Trusel et al., 2019; Brinschwitz et al., 2010; Proulx et al., 2014). lHb was shown to encode aversive experiences (Matsumoto and Hikosaka, 2007; Lazaridis et al., 2019) and prediction errors (Trusel et al., 2019; Kawai et al., 2015). Instead, the medial Hb (mHb) receives inputs from supracommissural septum, VTA, and locus coeruleus and projects to interpeduncular nucleus (IPN) that is connected with the raphe nuclei (Fore et al., 2018; Bianco and Wilson, 2009; Namboodiri et al., 2016; Hentall and Budhrani, 1990; Groenewegen et al., 1986). Most studies on mHb focus on its role in depression, anxiety, fear, addiction, and anhedonia (Yamaguchi et al., 2013; Shih et al., 2015; Frahm et al., 2011). Yet, little is known about the role mHb plays in operant learning.

Consistent with that of mammals, zebrafish studies highlight the role of Hb in learning and emotional behaviors. Based on neural connectivity and molecular characteristics, the zebrafish ventral Hb (vHb) and dorsal Hb (dHb) are homologous to mammalian lHb (Amo et al., 2010) and mHb (Agetsuma et al., 2010), respectively. Similar to taht of mammals, zebrafish Hb receives inputs from the hypothalamus (Turner et al., 2016), entopeduncular nucleus (vEN) (Amo et al., 2014), and median raphe (MR) (Turner et al., 2016). Zebrafish dHb projects to IPN, whereas vHb projects to the MR (Agetsuma et al., 2010; Amo et al., 2010, 2014; Chou et al., 2016). Ablating zebrafish vHb impairs active avoidance learning, without affecting the defensive behavior induced by classical fear conditioning (Amo et al., 2014). Alternatively, ablation of zebrafish dHb disrupts the execution of experience-dependent fear response (Lee et al., 2010; Agetsuma et al., 2010). Two sub-regions of dHb, the dorsolateral Hb (dlHb) and the mediodorsal Hb (mdHb), regulate behavioral flexibility during social conflict by differentially influencing animals' probability to win or lose. This regulation was proposed to be mediated through specific targeting of the IPN, which projects to the griseum centrale (Chou et al., 2016). Recent studies suggest further roles for dHb and vHb in

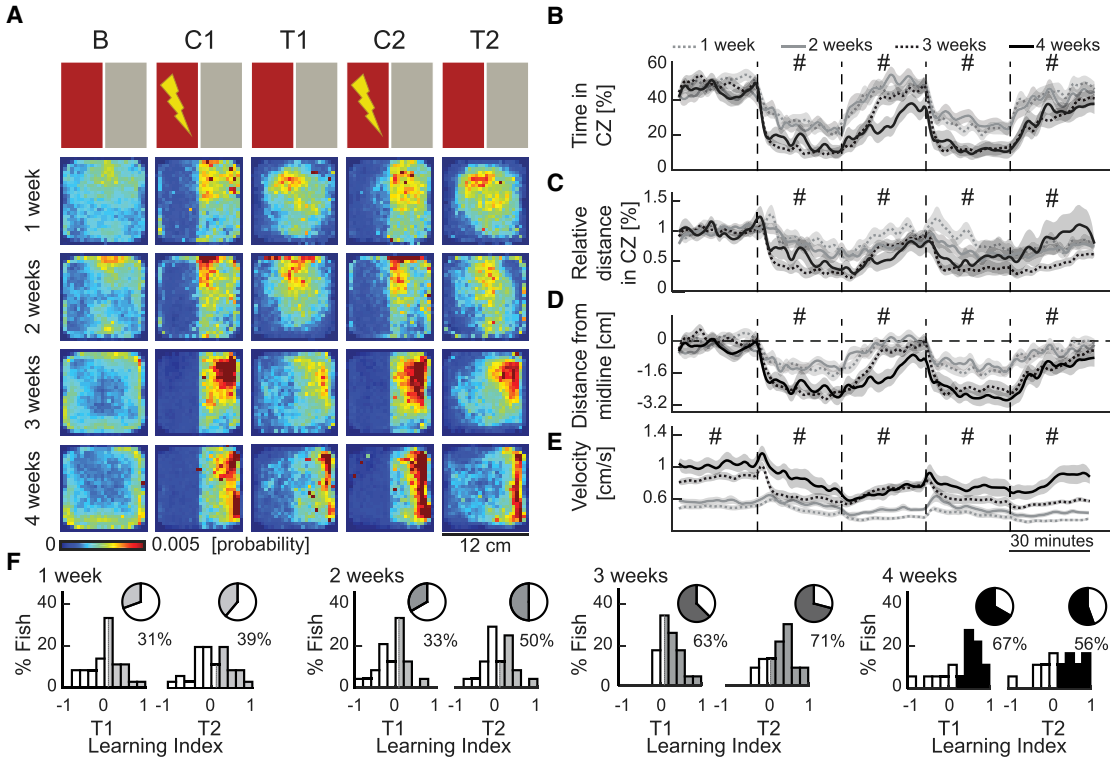

Figure 1. Juvenile Zebrafish Can Perform Conditioned Place Avoidance Learning with Increased Performance across Development

(A) The top row shows a schematic representation of the protocol. B, baseline; C1, conditioning 1; T1, test 1; C2, conditioning 2; T2, test 2. Consecutive rows show the heatmaps depicting the average density of zebrafish position for each experimental group: 1-week-old (n = 36), 2-week-old (n = 24), 3-week-old (n = 24), and 4-week-old (n = 18) zebrafish.

(B) Relative time spent in the conditioned zone (CZ).

(C) Relative distance of swimming in the CZ.

(D) Average distance of the animals away from the CZ. Dashed line indicates the midline.

(E) Average swim velocity.

(B–E) Line color and style indicate different age groups. Data displayed in 2-min bins; mean ± SEM; #, indicate statistical comparisons detailed in Figures S1E and S1F.

(F) Histograms of CPA learning indices during the two test sessions. The darker colors represent the animals classified as learners. The percentage of learners is in the pie chart. See also Figures S1 and S2.

behavioral flexibility, for recovering from (Duboué et al., 2017) or for coping with aversive experiences (Andalman et al., 2019). All these studies emphasize the involvement of the Hb in coordinating multiple neural processes, evaluating outcomes, and selecting optimal behaviors in response to experienced changes in the environment. However, it is less clear how changes in learned rules in cognitively demanding tasks are integrated in the brain and what role the Hb plays in this behavioral flexibility. Investigation of such cognitively demanding behaviors in transparent juvenile zebrafish would open new avenues for studying the neural basis of behavioral flexibility across widely dispersed brain regions.

RESULTS

Juvenile Zebrafish Can Perform Conditioned Place Avoidance with Increasing Performance across Development

To investigate the ontogeny of CPA learning, we focus on the first 4 weeks of development, during which zebrafish (i.e., *nacre* mutants with reduced pigmentation) (Lister et al., 1999) are relatively translucent and amenable for functional imaging of dorsal brain regions (Jetti et al., 2014; Fore et al., 2019; Vendrell-Llopis and Yaksi, 2015). During these first 4 weeks, we observed that the size of zebrafish increased significantly from the larval to juvenile stage (Figure S1B). The juvenile zebrafish at 3–4 weeks exhibit noticeable variability, compared to younger animals, both in size (Figure S1B) and swim velocity (Figure S1C). Using a custom-built behavioral setup (Figure S1A), we trained zebrafish in a CPA protocol, for which they received mildly aversive electric stimuli only when they entered the conditioned zone of the arena, marked by a red color presented from the bottom. The training was composed of a baseline session followed by two blocks of conditioning and test sessions (Figure 1A; Figure S1A). During the baseline, we observed no exploration bias of the arena (Figures 1A, 1B, and 1D). We quantified learning performance by using multiple measures, such as the reduction of the relative time spent (Figure 1B) and the relative distance of swim (Figure 1C) in the conditioned zone, as well as the average distance from the boundary between the conditioned and safe

zones (Figure 1D), which were used in previous studies (Millot et al., 2014, Valente et al., 2012). During conditioning sessions C1 and C2, zebrafish exhibited a significant decrease of time spent in the conditioned zone, at all developmental stages (Figures 1A and 1B; Figures S1E and S1F). However, only 3 and 4-week-old zebrafish retained a significant avoidance behavior during the test sessions, with 4-week-old animals performing significantly better than 3-week-old ones (Figures 1A and 1B; Figures S1E and S1F). These results were confirmed by all other complementary measures of learning (Figures 1C and 1D; Figures S1E and S1F). Consistent with previous studies (Müller and van Leeuwen, 2004), we observed a relationship between the swim velocity and the size of zebrafish (Figure S1C). All groups decreased their swimming velocity during the conditioning protocol (Figure 1E) and responded to the aversive stimuli with a transient speed increase (Figure S1D). We did not observe any significant difference between the CPA performance of wild-type zebrafish and *nacre* mutants with reduced pigmentation (Lister et al., 1999; Figures S2A–S2G). Finally, we showed that up to 70% of juvenile zebrafish at the third and fourth week of development exhibit learning indices significantly greater than chance levels (Figure 1F). To address a potential source of variability in performance, we investigated the relationship between CPA performance and animal size. Our results demonstrated that larger zebrafish exhibit better learning performance (Figure S1H). Altogether, these results show that juvenile zebrafish can perform CPA learning with increasing performance across development.

Comparing Operant Learning with Defensive Behaviors Elicited by Aversive Stimuli

To compare the defensive behaviors or potential stress elicited by aversive electric stimuli with the operant learning behavior, we designed a sham training protocol for 3- to 4-week-old, size-matched, juvenile zebrafish. To do this, we trained half of the animals with the CPA protocol, while in parallel a sham group was simultaneously exposed to the same aversive stimuli. To match the aversive experience in both groups, the mild electric stimuli of the sham group were precisely timed and dictated by the actions of their CPA-trained siblings in a neighboring behavioral arena with the same features (color, shape, and temperature). Because the sham animals' aversive experiences were independent of their behavior and solely controlled by the actions of their CPA-trained siblings, the sham group experienced the same aversive stimuli in a similar arena without the opportunity to learn (Figure 2A). As expected, the trained zebrafish learned the CPA task and avoided the conditioned zone successfully in all measures of learning (black traces, Figures 2B–2D). However, sham animals had no opportunity to learn (red traces, Figures 2B–2D). We observed that trained animals exhibited a lower swimming velocity than the sham group (Figure 2E). Hence, the reduction in speed was not merely due to the response of the animals to aversive stimuli but due to a change in behavioral strategy upon CPA learning. Both trained and sham animals exhibited freezing behavior (i.e., swimming less than 2 mm during 2 s) on average less than 0.5% of the time (Figure 2F), and both groups responded to the aversive shock with a transient increase in swim velocity (Figure 2G).

Next, we investigated the animals' behavior as zebrafish swam toward the visual boundary between the safe and conditioned zones, during sessions C2 and T2. We observed that most CPA-trained zebrafish took evasive action at the visual boundary and successfully avoided to enter into the conditioned zone (Figures 2H and 2I, black dots on the right hemisphere) or never approached the boundary (Figures 2H and 2I, black dots outside the right hemisphere). Conversely, the sham group did not perceive the visual boundary as relevant features of the environment and did not take evasive action (Figures 2H and 2I, red circles on the left hemisphere). The avoidance behaviors of trained and sham groups were significantly different for all iterations of various distances from the boundary (Figure S3A). Moreover, we confirmed that sham group exhibit significant differences in additional measures of learning, such as the reduction of swimming duration (Figure 2J) and distance (Figure S3B) in the conditioned zone upon each entry, as well as the total number of entries into the conditioned zone (Figure S3C). Altogether, these results highlight that juvenile zebrafish exhibit substantially different behaviors during CPA learning compared to defensive behaviors or potential stress elicited by aversive electric stimulation and that CPA learning behavior can be separated from defensive behaviors or stress.

CPA Performance and Memory Recall Improve across Multiple Training Sessions

Next, we asked whether zebrafish improve their performance across multiple training days and whether such training facilitates long-term learning and memory consolidation. To achieve this, we trained 4-week-old juvenile zebrafish across 4 consecutive days (Figure 3A). In line with our hypothesis, multi-day training improved the performance in all measurements of learning (Figures 3A–3D and 3F; Figures S4A–S4D), especially compared to training day 1 (Figure 1; Figures S4A–S4D). The percentage of animals classified as learners increased from 67% in day 1 up to 89% in the consecutive training days (Figure 3F). This increased learning index was also accompanied by a reduction in inter-individual variability of CPA performances (Figure 3F). Next, we investigated the memory recall after multi-day CPA training. To do this, we analyzed and compared the 10-min time windows during the switch from blank to the presentation of the recall pattern (boxes labeled B' and R' in Figures 3B and 3C). From the third day of training onward, we observed a transient but significant memory recall when CPA color cues were presented directly after the blank session. This was quantified by a reduced time spent (Figure 3G) and a reduced distance swim (Figure 3H) in the conditioned zone. We also observed that during the recall period, the zebrafish perceived the boundary between the color cues and took evasive action as they approached the boundary of the conditioned zone (Figure 3I, black arrow). The ratio of successful avoidance during recall significantly increased (Figure 3I) across multi-day training. We observed freezing on average less than 1% of the time, during multi-day training (Figure S4E). Our results demonstrated that the CPA performance of zebrafish improves across multiple training days and that zebrafish form long-term CPA memories.

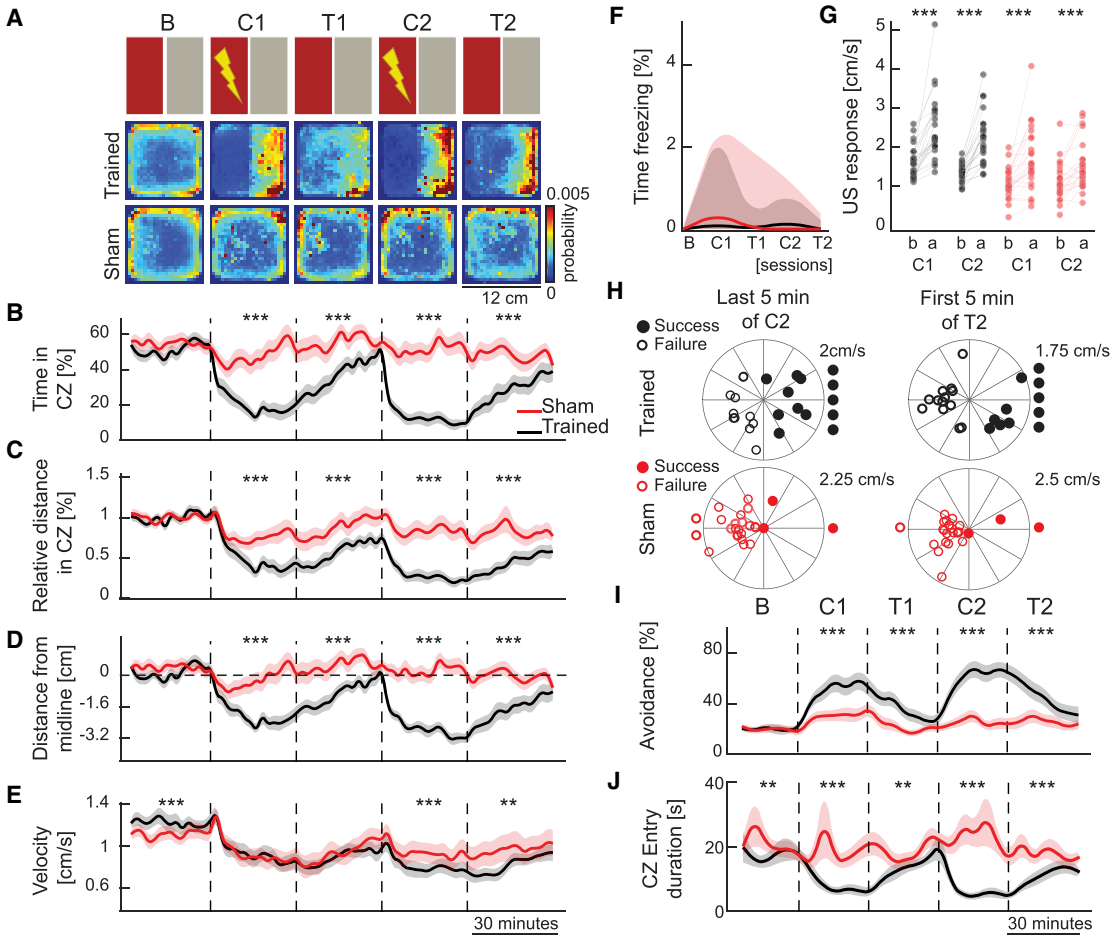

Figure 2. Comparing Operant Learning with Defensive Behaviors Elicited by Aversive Stimuli

(A) The top row shows a schematic representation of the protocol. Consecutive rows show the heatmaps depicting the average density of zebrafish position for trained (n = 25) and sham (n = 25) groups.

(B) Relative time spent in the CZ.

(C) Relative distance of swimming in the CZ.

(D) Average distance of the animals away from the CZ. Dashed line indicates the midline.

(E) Average swimming velocity of the zebrafish.

(B–E) Line colors indicate control (black) and sham (red) groups, 3- to 4-weeks old. Data are displayed in 2-min bins; mean ± SEM.

(F) Percentage of time that the zebrafish exhibit no swimming less than 2-mm during 2 s. Solid lines represent median, and shaded areas represent first and third quartiles.

(G) Average swimming velocity of the zebrafish, 1 sec before (b) and after (a) the delivery of aversive unconditioned stimuli (US).

(H) Zebrafish swimming direction near the boundary of CZ and safe zone (SZ), during the last 5 min of C2 (left) and first 5 min of T2 (right), in CPA-trained (top, black) and sham (bottom, red) groups. Each dot on the polar plot depicts the average swimming direction of one zebrafish during the 5 secs after encountering the CZ/SZ boundary. For each dot, the distance from the center encodes the average swimming velocity of the animal. Filled dots represent successful avoidance of zebrafish, and empty dots represent unsuccessful ones. Dots outside the polar plots represent animals that never entered the CZ (filled) or that never left the CZ (empty).

(I) Average ratio of successful avoidance over the protocol, divided in 5-min time bins (mean ± SEM).

(J) Average swim duration up on each entry to CZ; data displayed in 5-min time bins; mean ± SEM. ***p ≤ 0.001, **p ≤ 0.01, *p ≤ 0.05. Wilcoxon signed-rank test. See also Figure S3.

dlHb Ablation Leads to an Apparent Improvement of CPA Performance

dlHb ablation in adult zebrafish was shown to interfere with the execution of experience-dependent fear responses (Agetsuma et al., 2010). We hypothesized that dlHb ablation might also interfere with CPA learning. We achieved chemogenetic ablation of the dlHb by incubating 3 to 4-week-old juvenile pigmented zebrafish Tg(narp:GAL4VP16; UAS-E1b:NTR-mCherry) (Agetsuma et al., 2010) with 10 mM metronidazole (MTZ) (Figures 4A and 4B). Similar to adult zebrafish (Agetsuma et al., 2010), narp:Gal4 is expressed in dlHb neurons of juvenile zebrafish (Figures S5A–S5F; Video S1). More lateral narp:Gal4 expression in adults is due to sequential habenular neurogenesis across development (Fore et al., 2019). Next, we compared dlHb-ablated juvenile zebrafish with the control group in multi-day CPA training. To our surprise, we observed that dlHb-ablated

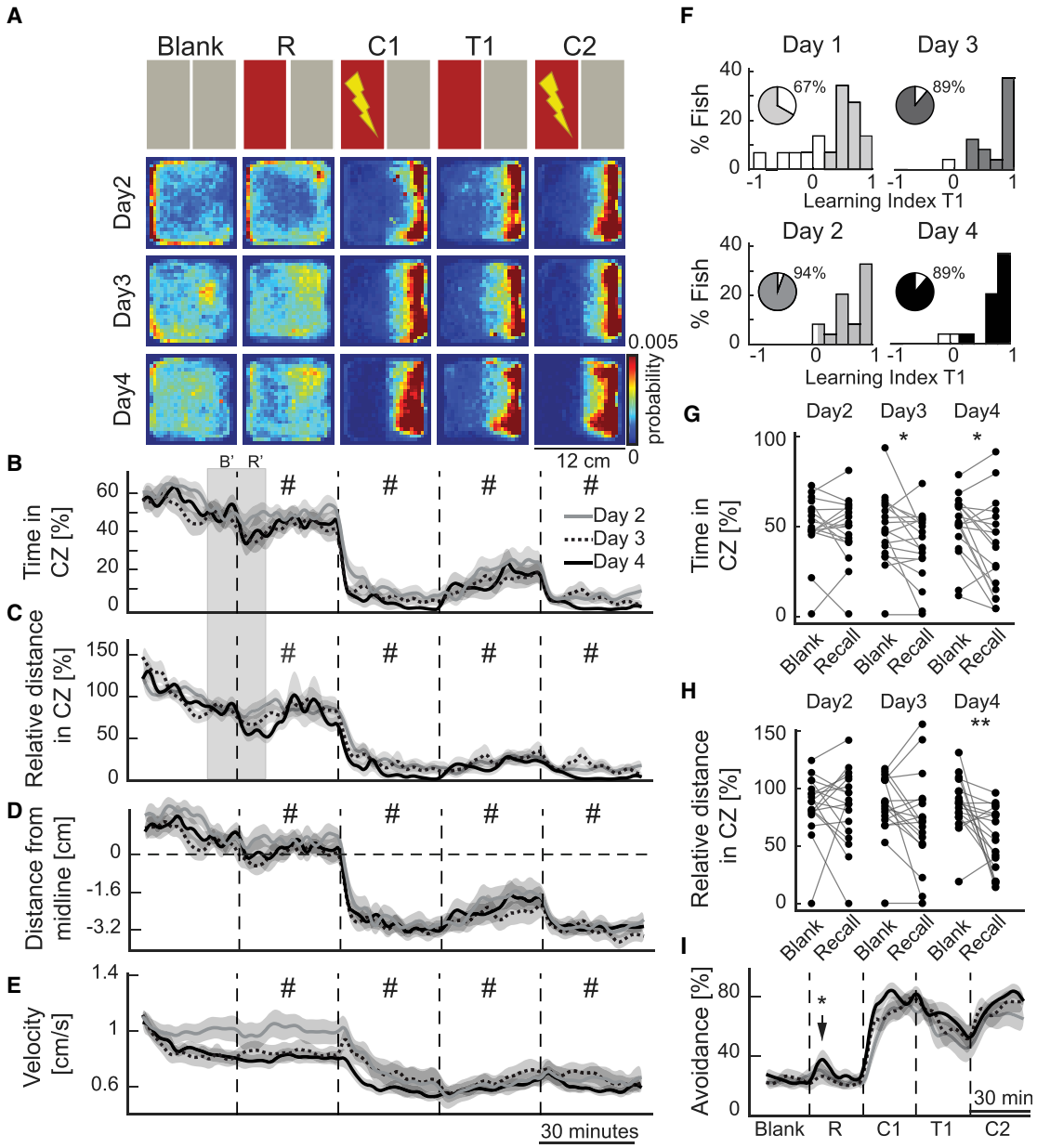

Figure 3. CPA Performance and Memory Recall Improve across Multi-day Training

(A) The top row shows a schematic representation of the protocol. Blank, baseline with no color cues; R, recall. The next rows show the heatmaps depicting the average density of zebrafish position during multiple training days (n = 18).

(B) Relative time spent in the CZ.

(C) Relative distance of swim in the CZ.

(D) Average distance of the animals away from the CZ. Dashed line indicates the animal being on the midline.

(E) Average swimming velocity of the zebrafish.

(B–E) Line colors and style indicate zebrafish performance during multiple training days in 4-week-old zebrafish. Data are displayed in 2-min bins; mean ± SEM; #, indicates significance comparisons, detailed in Figure S4A.

(F) Histograms of the learning indices during the test session, across multiple days of training. The darker colors represent the animals classified as learners. The percentage of learners is in the pie chart.

(G) Average time spent by the animal in the CZ during the last 10 min of the blank session (B') and in the first 10 min of the recall session (R').

(H) Relative distance of swim in the during B' and in R'. B' and R' periods are marked with the gray box in (B) and (C).

(I) Average ratio of successful avoidance over the course of the protocol, divided in 5-min time bins; mean ± SEM. ***p ≤ 0.001, **p ≤ 0.01, *p ≤ 0.05. (G, H, and K) Wilcoxon signed-rank test. See also Figure S4.

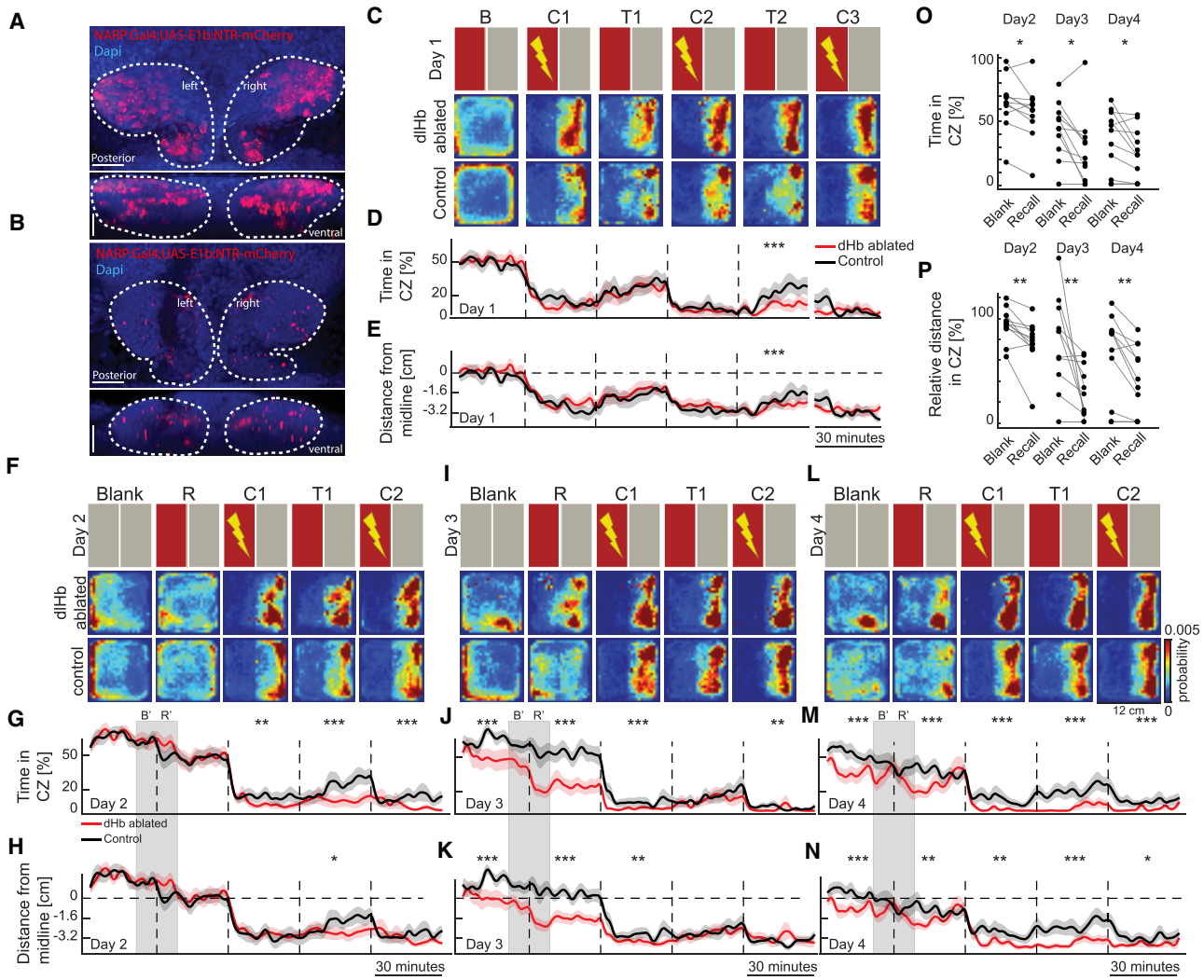

Figure 4. Dorsolateral Habenula Ablation Improves CPA Performance and Delays Memory Extinction

(A and B) Confocal microscopy images of Tg(narp:Gal4;UAS-E1b:NTR-mCherry) zebrafsh before (A) and after (B) metrodiniazole (MTZ) treatment. Dorsal (top) and coronal (bottom) views. Scale bars are 25 μm.

(C, F, I, and L) The top row shows a schematic representation of the protocol. The next rows show the heatmaps depicting the average density of zebrafish position for dlHb-ablated (n = 11) and control (n = 12) groups. (C) First day of training. (F) Second day of training. (I) Third day of training. (L) Fourth day of training.

(D, G, J, and M) Relative time spent in the CZ.

(E, H, K, and N) Average distance of the animals from the CZ. Dashed line indicates the midline.

(D, E, G, H, J, K, M, and N) Line colors indicate control (black) and dlHb-ablated (red) groups of 3- to 4-week-old zebrafish. Data are displayed in 2-min bins; mean ± SEM.

(O) Relative time spent by the dlHb-ablated zebrafish in the CZ during the last 10 min of the B' and in the first 10 min of the R'.

(P) Relative distance swam in the CZ during B' and R'. ***p ≤ 0.001, **p ≤ 0.01, *p ≤ 0.05. (D, E, G, H, J, K, M, and N) Wilcoxon rank-sum test; (O and P) Wilcoxon signed-rank test. See also Figure S5.

animals outperformed controls at the first training day and that their CPA performance remained higher than the control group over the consecutive training days (Figures 4C–4N). From the third training day onward, we also observed that dlHb-ablated animals exhibited robust CPA recall behavior (Figures 4O and 4P). Importantly, we did not observe freezing behavior in dlHb-ablated animals, more than 1% of the time, even after several days of CPA training (Figure S5G). These results suggest that dlHb ablation leads to an apparent improvement of CPA performance and a better memory recall, across multi-day training sessions.

The dlHb Is Important for Behavioral Flexibility during Reversal Learning

We hypothesized that one reason dlHb-ablated zebrafish performed better than control animals is an impairment in memory extinction. To test this, we introduced an extended extinction session (T3) after the CPA training. Consistent with our

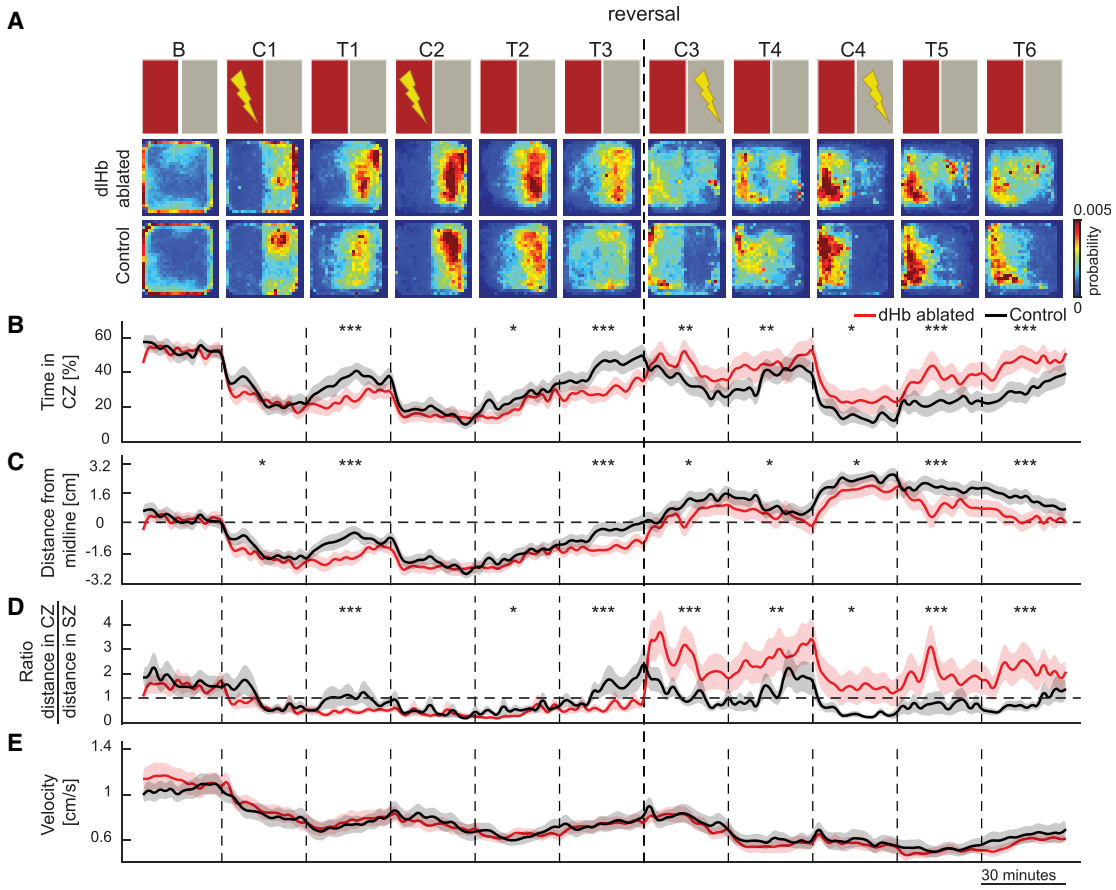

Figure 5. The Dorsolateral Habenula Is Important for Behavioral Flexibility during Reversal Learning

(A) The top row shows a schematic representation of the protocol. T3, test 3 (extinction test); C3, conditioning 3 (reversal learning); T4, test 4 (reversal learning test); C4, conditioning 4 (reversal learning); T5, test 5(reversal learning test); T6, test 6(reversal learning extinction test). The next rows show the heatmaps depicting the average density of zebrafish position for control (n = 21) and dlHb-ablated (n = 22) groups.

(B) Relative time spent in the CZ.

(C) Average distance of the animals away from the CZ. Dashed line indicates the midline.

(D) The ratio of swimming distance in CZ versus SZ.

(E) Average swimming velocity of the zebrafish.

(B–E) Line colors indicate control (black) and dlHb-ablated (red) groups of 3- to 4-week-old zebrafish. Data are displayed in 2-min bins; mean ± SEM. ***$p \leq 0.001$, **$p \leq 0.01$, *$p \leq 0.05$, Wilcoxon rank-sum test. See also Figure S5.

hypothesis, the dlHb-ablated zebrafish showed a significantly slower extinction rate of the avoidance behavior, during the extended extinction session (Figures 5A–5D). The slower memory extinction in dlHb animals can in principle be explained by an inefficient integration of new information with past experience. Because the dlHb-ablated animals performed better during the initial CPA protocol (Figures 4 and 5), we hypothesized that they might not integrate new information about the lack of aversive experience during the test sessions. Inspired by these results, we reversed the learning rule after the initial CPA training and paired the aversive stimuli with the part of the CPA arena marked with a gray visual cue (Figure 5, conditioning periods C3 and C4). In this reversal learning protocol, zebrafish were required to update their learned CPA behavior and relearn to associate the initial safe zone with the aversive experience. Excitingly, the dlHb-ablated zebrafish did significantly worse than control animals in reversal learning, quantified by all indicators of reversal learning performance (Figures 5A–5D). We observed no significant differences in the velocity of the dlHb-ablated group versus the control group (Figure 5E) and on average less than 1% of the time freezing behavior (Figure S5H). Both groups significantly increased their transient swimming velocity upon administration of the aversive stimulus (Figure S5I). Altogether, our results reveal that although dlHb ablation leads to better CPA performance, dlHb-ablated zebrafish exhibit an impaired ability to integrate new evidence into their past experience when tested in a memory extinction and reversal learning paradigm.

DISCUSSION

The zebrafish is becoming increasingly popular for studying diverse aspects of animal behavior (Orger et al., 2000; Huang

and Neuhauss, 2008; Koide et al., 2009; Burgess and Granato, 2007; Vendrell-Llopis and Yaksi, 2015; Kermen et al., 2020a), including complex behaviors, such as learning (Sison and Gerlai, 2010; Aoki et al., 2013; 2015; Chou et al., 2016; Lal et al., 2018; Valente et al., 2012; Yashina et al., 2019; Amo et al., 2014) and social interactions (Hinz and de Polavieja, 2017; Dreosti et al., 2015). While studying complex behaviors in adult zebrafish allows investigation of brain function in a fully mature brain, larval and juvenile zebrafish have the tremendous advantage of a small and relatively translucent brain, when it comes to studying brain activity (Thiele et al., 2014; Del Bene et al., 2010; Jetti et al., 2014; Dreosti et al., 2014; Naumann et al., 2016; Kawashima et al., 2016; Vendrell-Llopis and Yaksi, 2015). In line with previous studies (Valente et al., 2012; Yashina et al., 2019), we observed that from the third week of development, the learning performance of juvenile zebrafish becomes more robust and comparable to adults (Millot et al., 2014; Kedikian et al., 2013). All developmental stages exhibit inter-individual variability of CPA performance, similar to adult zebrafish for learned (Millot et al., 2014; Kedikian et al., 2013; Amo et al., 2014; Lal et al., 2018) or innate behaviors (Kermen et al., 2020a). Yet, our results demonstrated that the individual variability decreases as the CPA performance improves across development and across multiple days of training, reaching up to 90% of juvenile zebrafish with a learning index close to 1 at the fourth day of CPA training. We propose that using age- and size-matched 3- to 4-week-old zebrafish, and multi-day training is the best approach to reduce variability of CPA performance.

Quantifying animal behavior, especially operant learning, requires multiple and complementary approaches. Hence, we verified our CPA performance results by using various learning measures, such as the reduction of the relative time spent and the relative distance of swim in the conditioned zone, the average distance from the boundary of the conditioned zones, the duration and distance swim during each entry in the conditioned zone, and the number of entries in the conditioned zone. We also provided an avoidance measure based on animal swimming behaviors along the visual boundary between conditioned and safe zones. We suggest that combining these diverse learning measures in future studies will help interpretation of CPA learning results across different labs.

Our multi-day CPA training protocol revealed that 4-week-old zebrafish can recall CPA memories even after 24 h. Adult zebrafish were shown to recall memories encoded by telencephalic neural activity (Aoki et al., 2013), homologous to the mammalian cortex (Mueller and Wullimann, 2009), resembling the memory engrams described in mammals (Liu et al., 2012; Ramirez et al., 2014; Kitamura et al., 2017). Our results showed a long-term memory recall in juvenile zebrafish with small and relatively translucent brains that are amenable for functional brain imaging (Jetti et al., 2014; Fore et al., 2019; Vendrell-Llopis and Yaksi, 2015), at single neuron resolution. Future studies will be necessary to further investigate the neural basis of memory at different timescales and to understand how brain regions that are involved in short-term and long-term learning interact with each other to generate memory engrams.

The major brain regions required in operant learning, such as the amygdala and the hippocampus, are evolutionarily conserved across vertebrates (Lal et al., 2018; von Trotha et al., 2014; Mueller and Wullimann, 2009; Rodríguez et al., 2002; Elliott et al., 2017; Tosches et al., 2018). However, all these brain regions mature during vertebrate development by the addition of new cell types, new layers, or even entire brain structures (Donato et al., 2017; Frangeul et al., 2017; Sur and Leamey, 2001). Sequential addition of distinct neural layers across development was also shown in zebrafish telencephalon (Furlan et al., 2017; von Trotha et al., 2014) and Hb (Fore et al., 2019), which represents the developmentally expanding functionality of this ancestral cortico-limbic circuitry. Combined with all these earlier studies, our findings can therefore reflect an overall maturation of the zebrafish forebrain, allowing animals to integrate new information about their environment with their experiences and to evaluate them in a context-specific framework to make critical decisions.

An increasing number of studies use fear learning for studying the molecular and neural basis of learning (Kitamura et al., 2017; Redondo et al., 2014; Ramirez et al., 2014; Liu et al., 2012; Silva et al., 2016). However, it is not always easy to distinguish the effect of fear, stress, or defensive behaviors from learning, at the molecular and neuronal level in the brain. Here, we introduced an approach to compare and perhaps distinguish defensive behaviors or stress from learning. We argue that comparing the control group to the sham group would allow us to distinguish the learning-related processes in the brain from all other processes related to the animal's subjective experiences of the aversive stimuli. We propose that using very mild aversive stimuli and comparing trained animals with a sham group is a promising approach to be used in future studies for disentangling the neural processes underlying learning from defensive behaviors, stress, anxiety, or helplessness.

Studies in mammals established a direct role of the Hb in the prediction of learned outcomes (Trusel et al., 2019; Amo et al., 2014; Matsumoto and Hikosaka, 2007; Kawai et al., 2015; Matsumoto and Hikosaka, 2009) and negative motivational values (Wang et al., 2017; Hong et al., 2011; Lazaridis et al., 2019). Similarly, the zebrafish dHb and vHb were implicated in classical and operant learning (Agetsuma et al., 2010; Amo et al., 2014; Lee et al., 2010). At first glance, our results for improved CPA performance in dlHb-ablated zebrafish were surprising because they showed a significantly slower memory extinction rate than that of the control. In fact, the extinction of a memory is an essential component of learning (Singewald and Holmes, 2019; Felsenberg et al., 2018). The extinction of fear memories was proposed as a post-traumatic stress disorder (PTSD) therapy (Kida, 2019). Hence, comparing predicted outcomes with consequences is important for updating the previous memories with the new ones (Baker et al., 2017; Izquierdo et al., 2017). Our reversal learning experiments show that juvenile zebrafish exhibit such behavioral flexibility and can adapt to changing rules. However, dlHb-ablated zebrafish have difficulty adapting to changing CPA rule during reversal learning. Consequently, our results highlight an important role of dlHb in extinction of fear memories, which might have potential future implications for PTSD studies.

Our results show a key role for the zebrafish homolog of mammalian mHb in behavioral flexibility. We demonstrated

that ablation of zebrafish dlHb do not impact animals' ability to acquire a conditioned response, but it impairs animals' flexibility to update its learned response when the conditions or the rules are changed. Consistent with our findings, knockout mice lacking the *narp* gene, expressed both in the mouse mHb and the zebrafish dlHb (Agetsuma et al., 2010), were shown to succeed in instrumental conditioning but failed in a devaluation protocol, which required an adjustment of choices in the absence of rewards (Johnson et al., 2007). What mechanisms can underlie the effect of zebrafish dlHb (mammalian mHb) ablation in memory extinction and reversal learning? In mammals, lesioning mHb fibers, which modulate lHb activity (Viswanath et al., 2014), was shown to disrupt active avoidance learning (Wilcox et al., 1986). Hence, zebrafish dlHb might also regulate vHb activity, thereby influencing the function of vHb in learning. Such dlHb-vHb interactions, might co-exist, in parallel to well described innervations of dHb to different IPN domains (Agetsuma et al., 2010; Amo et al., 2014; Chou et al., 2016; Hong et al., 2013), which in turn project to the griseum centrale (Agetsuma et al., 2010; Chou et al., 2016) and MR (Agetsuma et al., 2010), regulating defensive behaviors.

Studies in primates highlight further roles for the Hb in adaptive behaviors (Baker et al., 2017; Kawai et al., 2015). In humans, impaired behavioral flexibility can lead to mood disorders (Lawson et al., 2017; Sartorius et al., 2010; Morris et al., 1999). In line with all these studies, our findings reveal an important and unexpected role for the mHb in optimizing animal behavior and complementing the lHb by providing the necessary behavioral flexibility in case of a mismatch between the predicted and the actual outcomes. In the future, it will be crucial to investigate the neural computations across widely dispersed brain regions of transparent juvenile zebrafish, which could further elucidate the role of the Hb and its input/output structures in behavioral flexibility and learning.

STAR★METHODS

Detailed methods are provided in the online version of this paper and include the following:

- KEY RESOURCES TABLE
- RESOURCE AVAILABILITY
  - Lead Contact
  - Materials Availability
  - Data and Code Availability
- EXPERIMENTAL MODEL AND SUBJECT DETAILS
- METHOD DETAILS
  - Behavioral setup
  - Experimental procedures
  - Baseline session
  - Blank session
  - Conditioning session
  - Test session
  - Metronidazole treatment
  - Immunohistochemistry and confocal imaging
- QUANTIFICATION AND STATISTICAL ANALYSIS
  - The learning index is defined as follows
  - Choice of statistical analysis

SUPPLEMENTAL INFORMATION

Supplemental Information can be found online at https://doi.org/10.1016/j.celrep.2020.108054.

ACKNOWLEDGMENTS

We thank Hitoshi Okamoto, Misha Ahrens (for transgenic lines), Siv Eggen, Vy Nguyen, Andreas Nygard (for technical assistance), Nathalie Jurisch-Yaksi and Stephanie Fore (for comments), and all Yaksi lab members (for stimulating discussions). This work was funded by ERC grant 335561 (F.P., R.P., and E.Y.), RCN FRIPRO grant 239973 (E.Y.), Kavli Foundation, and NTNU.

AUTHOR CONTRIBUTIONS

Conceptualization, F.P. and E.Y.; Methodology and data, F.P. and B.S.; Recording software, F.P. and R.P.; Data Analysis, F.P.; Investigation, all authors; Writing, F.P. and E.Y.; Review & Editing, all authors; Funding Acquisition and Supervision, E.Y.

DECLARATION OF INTERESTS

The authors declare no competing interests.

Received: March 26, 2020
Revised: June 23, 2020
Accepted: July 29, 2020
Published: August 25, 2020

REFERENCES

Agetsuma, M., Aizawa, H., Aoki, T., Nakayama, R., Takahoko, M., Goto, M., Sassa, T., Amo, R., Shiraki, T., Kawakami, K., et al. (2010). The habenula is crucial for experience-dependent modification of fear responses in zebrafish. Nat. Neurosci. *13*, 1354–1356.

Amo, R., Aizawa, H., Takahoko, M., Kobayashi, M., Takahashi, R., Aoki, T., and Okamoto, H. (2010). Identification of the zebrafish ventral habenula as a homolog of the mammalian lateral habenula. J. Neurosci. *30*, 1566–1574.

Amo, R., Fredes, F., Kinoshita, M., Aoki, R., Aizawa, H., Agetsuma, M., Aoki, T., Shiraki, T., Kakinuma, H., Matsuda, M., et al. (2014). The habenulo-raphe serotonergic circuit encodes an aversive expectation value essential for adaptive active avoidance of danger. Neuron *84*, 1034–1048.

Andalman, A.S., Burns, V.M., Lovett-Barron, M., Broxton, M., Poole, B., Yang, S.J., Grosenick, L., Lerner, T.N., Chen, R., Benster, T., et al. (2019). Neuronal Dynamics Regulating Brain and Behavioral State Transitions. Cell *177*, 970–985.e20.

Aoki, T., Kinoshita, M., Aoki, R., Agetsuma, M., Aizawa, H., Yamazaki, M., Takahoko, M., Amo, R., Arata, A., Higashijima, S., et al. (2013). Imaging of neural ensemble for the retrieval of a learned behavioral program. Neuron *78*, 881–894.

Aoki, R., Tsuboi, T., and Okamoto, H. (2015). Y-maze avoidance: an automated and rapid associative learning paradigm in zebrafish. Neurosci. Res. *91*, 69–72.

Baker, P.M., Oh, S.E., Kidder, K.S., and Mizumori, S.J. (2015). Ongoing behavioral state information signaled in the lateral habenula guides choice flexibility in freely moving rats. Front. Behav. Neurosci. *9*, 295.

Baker, P.M., Raynor, S.A., Francis, N.T., and Mizumori, S.J. (2017). Lateral habenula integration of proactive and retroactive information mediates behavioral flexibility. Neuroscience *345*, 89–98.

Bechard, A.R., LaCrosse, A., Namba, M.D., Jackson, B., and Knackstedt, L.A. (2018). Impairments in reversal learning following short access to cocaine self-administration. Drug Alcohol Depend. *192*, 239–244.

Bianco, I.H., and Wilson, S.W. (2009). The habenular nuclei: a conserved asymmetric relay station in the vertebrate brain. Philos. Trans. R. Soc. Lond. B Biol. Sci. *364*, 1005–1020.

Brinschwitz, K., Dittgen, A., Madai, V.I., Lommel, R., Geisler, S., and Veh, R.W. (2010). Glutamatergic axons from the lateral habenula mainly terminate on GABAergic neurons of the ventral midbrain. Neuroscience *168*, 463–476.

Burgess, H.A., and Granato, M. (2007). Sensorimotor gating in larval zebrafish. J. Neurosci. *27*, 4984–4994.

Chou, M.Y., Amo, R., Kinoshita, M., Cherng, B.W., Shimazaki, H., Agetsuma, M., Shiraki, T., Aoki, T., Takahoko, M., Yamazaki, M., et al. (2016). Social conflict resolution regulated by two dorsal habenular subregions in zebrafish. Science *352*, 87–90.

Del Bene, F., Wyart, C., Robles, E., Tran, A., Looger, L., Scott, E.K., Isacoff, E.Y., and Baier, H. (2010). Filtering of visual information in the tectum by an identified neural circuit. Science *330*, 669–673.

Donato, F., Jacobsen, R.I., Moser, M.B., and Moser, E.I. (2017). Stellate cells drive maturation of the entorhinal-hippocampal circuit. Science *355*, eaai8178.

Dreosti, E., Vendrell Llopis, N., Carl, M., Yaksi, E., and Wilson, S.W. (2014). Left-right asymmetry is required for the habenulae to respond to both visual and olfactory stimuli. Curr. Biol. *24*, 440–445.

Dreosti, E., Lopes, G., Kampff, A.R., and Wilson, S.W. (2015). Development of social behavior in young zebrafish. Front. Neural Circuits *9*, 39.

Duboué, E.R., Hong, E., Eldred, K.C., and Halpern, M.E. (2017). Left Habenular Activity Attenuates Fear Responses in Larval Zebrafish. Curr. Biol. *27*, 2154–2162.e3.

Elliott, S.B., Harvey-Girard, E., Giassi, A.C., and Maler, L. (2017). Hippocampal-like circuitry in the pallium of an electric fish: Possible substrates for recursive pattern separation and completion. J. Comp. Neurol. *525*, 8–46.

Felsenberg, J., Jacob, P.F., Walker, T., Barnstedt, O., Edmondson-Stait, A.J., Pleijzier, M.W., Otto, N., Schlegel, P., Sharifi, N., Perisse, E., et al. (2018). Integration of Parallel Opposing Memories Underlies Memory Extinction. Cell *175*, 709–722.e15.

Fore, S., Palumbo, F., Pelgrims, R., and Yaksi, E. (2018). Information processing in the vertebrate habenula. Semin. Cell Dev. Biol. *78*, 130–139.

Fore, S., Cosacak, M.I., Verdugo, C.D., Kizil, C., and Yaksi, E. (2019). Functional properties of habenular neurons are determined by developmental stage and sequential neurogenesis. bioRxiv. https://doi.org/10.1101/722462.

Frahm, S., Slimak, M.A., Ferrarese, L., Santos-Torres, J., Antolin-Fontes, B., Auer, S., Filkin, S., Pons, S., Fontaine, J.F., Tsetlin, V., et al. (2011). Aversion to nicotine is regulated by the balanced activity of β4 and α5 nicotinic receptor subunits in the medial habenula. Neuron *70*, 522–535.

Frangeul, L., Kehayas, V., Sanchez-Mut, J.V., Fièvre, S., Krishna-K, K., Pouchelon, G., Telley, L., Bellone, C., Holtmaat, A., Gräff, J., et al. (2017). Input-dependent regulation of excitability controls dendritic maturation in somatosensory thalamocortical neurons. Nat. Commun. *8*, 2015.

Furlan, G., Cuccioli, V., Vuillemin, N., Dirian, L., Muntasell, A.J., Coolen, M., Dray, N., Bedu, S., Houart, C., Beaurepaire, E., et al. (2017). Life-Long Neurogenic Activity of Individual Neural Stem Cells and Continuous Growth Establish an Outside-In Architecture in the Teleost Pallium. Curr. Biol. *27*, 3288–3301.e3.

George, S.A., Rodriguez-Santiago, M., Riley, J., Abelson, J.L., Floresco, S.B., and Liberzon, I. (2015). Alterations in cognitive flexibility in a rat model of post-traumatic stress disorder. Behav. Brain Res. *286*, 256–264.

Groenewegen, H.J., Ahlenius, S., Haber, S.N., Kowall, N.W., and Nauta, W.J.H. (1986). Cytoarchitecture, fiber connections, and some histochemical aspects of the interpeduncular nucleus in the rat. J. Comp. Neurol. *249*, 65–102.

Hadar, R., and Menzel, R. (2010). Memory formation in reversal learning of the honeybee. Front. Behav. Neurosci. *4*, 186.

Hentall, I.D., and Budhrani, V.M. (1990). The interpeduncular nucleus excites the on-cells and inhibits the off-cells of the nucleus raphe magnus. Brain Res. *522*, 322–324.

Hinz, R.C., and de Polavieja, G.G. (2017). Ontogeny of collective behavior reveals a simple attraction rule. Proc. Natl. Acad. Sci. USA *114*, 2295–2300.

Hong, S., Jhou, T.C., Smith, M., Saleem, K.S., and Hikosaka, O. (2011). Negative reward signals from the lateral habenula to dopamine neurons are mediated by rostromedial tegmental nucleus in primates. J. Neurosci. *31*, 11457–11471.

Hong, E., Santhakumar, K., Akitake, C.A., Ahn, S.J., Thisse, C., Thisse, B., Wyart, C., Mangin, J.M., and Halpern, M.E. (2013). Cholinergic left-right asymmetry in the habenulo-interpeduncular pathway. Proc. Natl. Acad. Sci. USA *110*, 21171–21176.

Huang, Y.Y., and Neuhauss, S.C. (2008). The optokinetic response in zebrafish and its applications. Front. Biosci. *13*, 1899–1916.

Izquierdo, A., Brigman, J.L., Radke, A.K., Rudebeck, P.H., and Holmes, A. (2017). The neural basis of reversal learning: An updated perspective. Neuroscience *345*, 12–26.

Jetti, S.K., Vendrell-Llopis, N., and Yaksi, E. (2014). Spontaneous activity governs olfactory representations in spatially organized habenular microcircuits. Curr. Biol. *24*, 434–439.

Johnson, A.W., Crombag, H.S., Takamiya, K., Baraban, J.M., Holland, P.C., Huganir, R.L., and Reti, I.M. (2007). A selective role for neuronal activity regulated pentraxin in the processing of sensory-specific incentive value. J. Neurosci. *27*, 13430–13435.

Kawai, T., Yamada, H., Sato, N., Takada, M., and Matsumoto, M. (2015). Roles of the Lateral Habenula and Anterior Cingulate Cortex in Negative Outcome Monitoring and Behavioral Adjustment in Nonhuman Primates. Neuron *88*, 792–804.

Kawashima, T., Zwart, M.F., Yang, C.T., Mensh, B.D., and Ahrens, M.B. (2016). The Serotonergic System Tracks the Outcomes of Actions to Mediate Short-Term Motor Learning. Cell *167*, 933–946.e20.

Kedikian, X., Faillace, M.P., and Bernabeu, R. (2013). Behavioral and molecular analysis of nicotine-conditioned place preference in zebrafish. PLoS One *8*, e69453.

Kermen, F., Darnet, L., Wiest, C., Palumbo, F., Bechert, J., Uslu, O., and Yaksi, E. (2020a). Stimulus-specific behavioral responses of zebrafish to a large range of odors exhibit individual variability. BMC Biol. *18*, 66.

Kermen, F., Lal, P., Faturos, N.G., and Yaksi, E. (2020b). Interhemispheric connections between olfactory bulbs improve odor detection. PLoS Biol. *18*, e3000701.

Kida, S. (2019). Reconsolidation/destabilization, extinction and forgetting of fear memory as therapeutic targets for PTSD. Psychopharmacology (Berl.) *236*, 49–57.

Kitamura, T., Ogawa, S.K., Roy, D.S., Okuyama, T., Morrissey, M.D., Smith, L.M., Redondo, R.L., and Tonegawa, S. (2017). Engrams and circuits crucial for systems consolidation of a memory. Science *356*, 73–78.

Koide, T., Miyasaka, N., Morimoto, K., Asakawa, K., Urasaki, A., Kawakami, K., and Yoshihara, Y. (2009). Olfactory neural circuitry for attraction to amino acids revealed by transposon-mediated gene trap approach in zebrafish. Proc. Natl. Acad. Sci. USA *106*, 9884–9889.

Lal, P., Tanabe, H., Suster, M.L., Ailani, D., Kotani, Y., Muto, A., Itoh, M., Iwasaki, M., Wada, H., Yaksi, E., and Kawakami, K. (2018). Identification of a neuronal population in the telencephalon essential for fear conditioning in zebrafish. BMC Biol. *16*, 45.

Lawson, R.P., Nord, C.L., Seymour, B., Thomas, D.L., Dayan, P., Pilling, S., and Roiser, J.P. (2017). Disrupted habenula function in major depression. Mol. Psychiatry *22*, 202–208.

Lazaridis, I., Tzortzi, O., Weglage, M., Märtin, A., Xuan, Y., Parent, M., Johansson, Y., Fuzik, J., Fürth, D., Fenno, L.E., et al. (2019). A hypothalamus-habenula circuit controls aversion. Mol. Psychiatry *24*, 1351–1368.

Lee, A., Mathuru, A.S., Teh, C., Kibat, C., Korzh, V., Penney, T.B., and Jesuthasan, S. (2010). The habenula prevents helpless behavior in larval zebrafish. Curr. Biol. *20*, 2211–2216.

Lister, J.A., Robertson, C.P., Lepage, T., Johnson, S.L., and Raible, D.W. (1999). nacre encodes a zebrafish microphthalmia-related protein that regulates neural-crest-derived pigment cell fate. Development *126*, 3757–3767.

Liu, X., Ramirez, S., Pang, P.T., Puryear, C.B., Govindarajan, A., Deisseroth, K., and Tonegawa, S. (2012). Optogenetic stimulation of a hippocampal engram activates fear memory recall. Nature *484*, 381–385.

Matsumoto, M., and Hikosaka, O. (2007). Lateral habenula as a source of negative reward signals in dopamine neurons. Nature *447*, 1111–1115.

Matsumoto, M., and Hikosaka, O. (2009). Two types of dopamine neuron distinctly convey positive and negative motivational signals. Nature *459*, 837–841.

Millot, S., Cerqueira, M., Castanheira, M.F., Øverli, Ø., Martins, C.I.M., and Oliveira, R.F. (2014). Use of conditioned place preference/avoidance tests to assess affective states in fish. Appl. Anim. Behav. Sci. *154*, 104–111.

Morris, J.S., Smith, K.A., Cowen, P.J., Friston, K.J., and Dolan, R.J. (1999). Covariation of activity in habenula and dorsal raphé nuclei following tryptophan depletion. Neuroimage *10*, 163–172.

Mueller, T., and Wullimann, M.F. (2009). An evolutionary interpretation of teleostean forebrain anatomy. Brain Behav. Evol. *74*, 30–42.

Müller, U.K., and van Leeuwen, J.L. (2004). Swimming of larval zebrafish: ontogeny of body waves and implications for locomotory development. J. Exp. Biol. *207*, 853–868.

Namboodiri, V.M., Rodriguez-Romaguera, J., and Stuber, G.D. (2016). The habenula. Curr. Biol. *26*, R873–R877.

Naumann, E.A., Fitzgerald, J.E., Dunn, T.W., Rihel, J., Sompolinsky, H., and Engert, F. (2016). From Whole-Brain Data to Functional Circuit Models: The Zebrafish Optomotor Response. Cell *167*, 947–960.e20.

Orger, M.B., Smear, M.C., Anstis, S.M., and Baier, H. (2000). Perception of Fourier and non-Fourier motion by larval zebrafish. Nat. Neurosci. *3*, 1128–1133.

Proulx, C.D., Hikosaka, O., and Malinow, R. (2014). Reward processing by the lateral habenula in normal and depressive behaviors. Nat. Neurosci. *17*, 1146–1152.

Ramirez, S., Tonegawa, S., and Liu, X. (2014). Identification and optogenetic manipulation of memory engrams in the hippocampus. Front. Behav. Neurosci. *7*, 226.

Redondo, R.L., Kim, J., Arons, A.L., Ramirez, S., Liu, X., and Tonegawa, S. (2014). Bidirectional switch of the valence associated with a hippocampal contextual memory engram. Nature *513*, 426–430.

Remijnse, P.L., Nielen, M.M., van Balkom, A.J., Hendriks, G.J., Hoogendijk, W.J., Uylings, H.B., and Veltman, D.J. (2009). Differential frontal-striatal and paralimbic activity during reversal learning in major depressive disorder and obsessive-compulsive disorder. Psychol. Med. *39*, 1503–1518.

Rodríguez, F., López, J.C., Vargas, J.P., Broglio, C., Gómez, Y., and Salas, C. (2002). Spatial memory and hippocampal pallium through vertebrate evolution: insights from reptiles and teleost fish. Brain Res. Bull. *57*, 499–503.

Sartorius, A., Kiening, K.L., Kirsch, P., von Gall, C.C., Haberkorn, U., Unterberg, A.W., Henn, F.A., and Meyer-Lindenberg, A. (2010). Remission of major depression under deep brain stimulation of the lateral habenula in a therapy-refractory patient. Biol. Psychiatry *67*, e9–e11.

Schindelin, J., Arganda-Carreras, I., Frise, E., Kaynig, V., Longair, M., Pietzsch, T., Preibisch, S., Rueden, C., Saalfeld, S., Schmid, B., et al. (2012). Fiji: an open-source platform for biological-image analysis. Nat. Methods *9*, 676–682.

Shih, P.Y., McIntosh, J.M., and Drenan, R.M. (2015). Nicotine Dependence Reveals Distinct Responses from Neurons and Their Resident Nicotinic Receptors in Medial Habenula. Mol. Pharmacol. *88*, 1035–1044.

Silva, B.A., Gross, C.T., and Gräff, J. (2016). The neural circuits of innate fear: detection, integration, action, and memorization. Learn. Mem. *23*, 544–555.

Singewald, N., and Holmes, A. (2019). Rodent models of impaired fear extinction. Psychopharmacology (Berl.) *236*, 21–32.

Sison, M., and Gerlai, R. (2010). Associative learning in zebrafish (Danio rerio) in the plus maze. Behav. Brain Res. *207*, 99–104.

Skinner, B.F. (1981). Selection by consequences. Science *213*, 501–504.

Skinner, B.F. (1984). The evolution of behavior. J. Exp. Anal. Behav. *41*, 217–221.

Stamatakis, A.M., and Stuber, G.D. (2012). Activation of lateral habenula inputs to the ventral midbrain promotes behavioral avoidance. Nat. Neurosci. *15*, 1105–1107.

Sur, M., and Leamey, C.A. (2001). Development and plasticity of cortical areas and networks. Nat. Rev. Neurosci. *2*, 251–262.

Thiele, T.R., Donovan, J.C., and Baier, H. (2014). Descending control of swim posture by a midbrain nucleus in zebrafish. Neuron *83*, 679–691.

Tosches, M.A., Yamawaki, T.M., Naumann, R.K., Jacobi, A.A., Tushev, G., and Laurent, G. (2018). Evolution of pallium, hippocampus, and cortical cell types revealed by single-cell transcriptomics in reptiles. Science *360*, 881–888.

Trusel, M., Nuno-Perez, A., Lecca, S., Harada, H., Lalive, A.L., Congiu, M., Takemoto, K., Takahashi, T., Ferraguti, F., and Mameli, M. (2019). Punishment-Predictive Cues Guide Avoidance through Potentiation of Hypothalamus-to-Habenula Synapses. Neuron *102*, 120–127.e4.

Turner, K.J., Hawkins, T.A., Yáñez, J., Anadón, R., Wilson, S.W., and Folgueira, M. (2016). Afferent Connectivity of the Zebrafish Habenulae. Front. Neural Circuits *10*, 30.

Valente, A., Huang, K.H., Portugues, R., and Engert, F. (2012). Ontogeny of classical and operant learning behaviors in zebrafish. Learn. Mem. *19*, 170–177.

Vendrell-Llopis, N., and Yaksi, E. (2015). Evolutionary conserved brainstem circuits encode category, concentration and mixtures of taste. Sci. Rep. *5*, 17825.

Viswanath, H., Carter, A.Q., Baldwin, P.R., Molfese, D.L., and Salas, R. (2014). The medial habenula: still neglected. Front. Hum. Neurosci. *7*, 931.

Vladimirov, N., Mu, Y., Kawashima, T., Bennett, D.V., Yang, C.T., Looger, L.L., Keller, P.J., Freeman, J., and Ahrens, M.B. (2014). Light-sheet functional imaging in fictively behaving zebrafish. Nat. Methods *11*, 883–884.

von Trotha, J.W., Vernier, P., and Bally-Cuif, L. (2014). Emotions and motivated behavior converge on an amygdala-like structure in the zebrafish. Eur. J. Neurosci. *40*, 3302–3315.

Wang, D., Li, Y., Feng, Q., Guo, Q., Zhou, J., and Luo, M. (2017). Learning shapes the aversion and reward responses of lateral habenula neurons. eLife *6*, e23045.

Wilcox, K.S., Christoph, G.R., Double, B.A., and Leonzio, R.J. (1986). Kainate and electrolytic lesions of the lateral habenula: effect on avoidance responses. Physiol. Behav. *36*, 413–417.

Yamaguchi, T., Danjo, T., Pastan, I., Hikida, T., and Nakanishi, S. (2013). Distinct roles of segregated transmission of the septo-habenular pathway in anxiety and fear. Neuron *78*, 537–544.

Yashina, K., Tejero-Cantero, Á., Herz, A., and Baier, H. (2019). Zebrafish exploit visual cues and geometric relationships to form a spatial memory. iScience *19*, 119–134.

STAR★METHODS

KEY RESOURCES TABLE

REAGENT or RESOURCE	SOURCE	IDENTIFIER
Chemicals, Peptides, and Recombinant Proteins		
Metronidazole (MTZ)	Sigma-Aldrich	Cat# M1547
Dimethyl sulfoxide (DMSO)	Sigma-Aldrich	Cat# 276855
Phosphate-buffered saline (PBS)	Thermo Fisher Scientific	Cat# BR0014G
Formaldehyde	Sigma-Aldrich	Cat# F8775
Bovine Serum Albumin Fraction V	Applichem/Panreac	Cat# A1391.0100
LMP Agarose	Fisher Scientific	Cat# 16520100
MS222 (Tricaine methanesulfonate)	Sigma-Aldrich	Cat# E10521
DAPI	Thermo Fisher Scientific	Cat# P36931
Goat Serum	Sigma-Aldrich	Cat# G9023
Triton X-100	Merck	Cat# 108643
Glycerol	Sigma-Aldrich	Cat# 1.04092
Experimental Models: Organisms/Strains		
Tg(elavl3:GCaMP6s)	Vladimirov et al., 2014	ZFIN ID: ZDB-ALT-141023-1, RRID:ZFIN_ZDB-ALT-141023-1
Tg(narp:GAL4VP16)	Agetsuma et al., 2010	ZFIN ID: ZDB-ALT-110215-5
Tg(UAS-E1b:NTR-mCherry)	Agetsuma et al., 2010	ZFIN ID: ZDB-ALT-070316-1
AB Wildtype Zebrafish	EZRC (https://www.ezrc.kit.edu/)	ZFIN ID: ZDB-GENO-960809-7
Software and Algorithms		
Fiji/ImageJ	Schindelin et al., 2012	N/A
MATLAB 2019b	https://se.mathworks.com/	N/A
Other		
Open CV3.0	https://opencv.org/opencv-3-0/	N/A
QtCreator5.2	https://www.qt.io/	N/A
Confocal microscope (20x plan NA 0.8 objective)	Zeiss	Examiner Z1
Confocal microscope (20x plan NA 1.0, Plan-Apochromat)	Zeiss	Examiner Z1

RESOURCE AVAILABILITY

Lead Contact

Further information and requests for resources and reagents should be directed to and will be fulfilled by the Lead Contact, Emre Yaksi (emre.yaksi@ntnu.no)

Materials Availability

This study did not generate new unique reagents.

Data and Code Availability

All analyses were performed with Fiji/ImageJ (Schindelin et al., 2012) and MATLAB 2019a as indicated in the results sections. All custom MATLAB scripts are available upon request.

EXPERIMENTAL MODEL AND SUBJECT DETAILS

The animal facilities and maintenance of the zebrafish, Danio rerio, were approved by the NFSA (Norwegian Food Safety Authority). Fish were kept in 3.5-l tanks in a Techniplast Zebtech Multilinking system at constant conditions: 28°C, pH 7 and 600μSiemens, at a 14:10 hour light/dark cycle to simulate optimal natural breeding conditions. Fish received a normal diet of dry food (SDS 100-400, dependent of age) two times/day and Artemia nauplii once a day (Grade0, platinum Label, Argent Laboratories, Redmond, USA). For the experiments shown in Figures 1, 2, 3, and S2 we used Tg(elavl3:GCaMP6s) (Vladimirov et al., 2014) pigmentless "nacre"

zebrafish, in AB background. For the control experiment shown in Figure S2 we also used three-week-old pigmented AB wild-type zebrafish. Experimental animals included in Figure 1 are of four age groups: one-week-old, two-week-old, three-week-old and four-week-old. Each of these groups had a variability of plus or minus two days. For the experiments shown in Figure 2 we used three- to four-week-old, size-matched, juvenile zebrafish. Experiments in Figure S2 include three-weeks old animals. We used four-week-old zebrafish for the long-term training investigated in Figure 3. For the experiments shown in Figures 4 and 5 we used three- to four-week-old Tg(narp:GAL4VP16);Tg(UAS-E1b:NTR-mCherry) (Agetsuma et al., 2010) double transgenic fish and siblings not expressing NTR-mCherry protein as controls, in pigmented AB wild-type background. All experimental procedures performed were in accordance with the directive 2010/63/EU of the European Parliament and the Council of the European Union and the Norwegian Food Safety Authorities.

METHOD DETAILS

Behavioral setup

Custom-made real-time tracking software was implemented to track six zebrafish simultaneously, using the OpenCV 3.0 library and the QtCreator5.2 developing platform. A microcontroller controls six integrated circuits to deliver electrical stimulation to each individual arena. Each current pulse has a duration of 10 ms and an amplitude of approximately 1.2 mA. This results in a current density of approximately 0.1 mA/cm using tungsten electrodes. A pulse of current is delivered every 740 ms, resulting in a delivery frequency of 1.33 Hz. The aversive stimulus is administered to the fish only when it is located inside the conditioned zone. The visual stimulus is presented from the bottom of the arena using a horizontally positioned LCD monitor. Each of the six arenas was divided into 2 equal parts with red and gray colors with matched luminosity. A Manta 235B camera was used to monitor animal behavior at 15 fps. Experiments were conducted in Gosselin square Petri dishes 120mm x 120mm x 15.8 mm with opaque side walls. The entire behavioral setup was enclosed in a temperature-controlled black isolation box to prevent any external interference. The water temperature during training was kept at 26°C. A schematic of the behavioral setup is shown in Figure S1A.

Experimental procedures

One fish per arena was placed in the behavioral setup between 09:00 and 11:00 am, after the morning feeding, and the experiment was started immediately. Every animal was used only in one specific protocol once. All the behavioral protocols performed in this work are composed of the following sessions that were used in various combinations:

Baseline session

the animal's position was monitored and recorded for 60 minutes, while the color pattern was displayed to the animal.

Blank session

position was monitored and recorded for 30 minutes, but no color pattern was presented to the animal; the arena was entirely covered by a uniform gray color.

Conditioning session

position was monitored and recorded for 30 minutes. Only when the zebrafish enters the conditioned zone a mildly aversive weak (10 ms, 1.2 mA) electric stimulus was delivered at 1.33 Hz.

Test session

position was monitored and recorded for 30 minutes, while the color pattern was displayed to the animal.

In Figures 1, 2, 3, and 4, the "conditioned zone" was always associated with the left half of the arena. In Figures 1, 3, and 4 the conditioned side of the arena was always associated with the red color. In the experiment presented in Figure 2 half of the animals were trained against the red color pattern, the other half against the gray color pattern. We observed no substantial differences in this two groups and combined both groups for data analysis. Each of these conditions had the corresponding sham control animals. The reversal protocol in Figure 5 was achieved by first conditioning the animals against the left/red side of the arena. During the third and fourth conditioning session the aversive stimulus was experienced only on the right/gray side of the arena. For the multi-day CPA training experiments shown in Figures 3 and 4 each individual animal, at the end of each training day, was transferred to a Petri dish containing fresh artificial fish water and they were fed with dry food and placed back in the incubator. The water was changed at least one additional time before the next day experiment.

Metronidazole treatment

To ablate the neurons of dlHb, Tg(narp:GAL4VP16; UAS-E1b:NTR-mCherry) zebrafish were treated with 10mM metronidazole (MTZ, Sigma-Aldrich) for 24h followed by a washout period of at least 12h, protocol adapted from Agetsuma et al. (2010). The treatment was started two days prior the behavioral protocol. The fish were placed, in groups of three, in a Petri dish containing 50ml of 10mM MTZ +250 μl of DMSO. Control group was subjected to the same treatment. The fish were kept in the 28°C incubator, covered in aluminum foil, for 24h. The next day the fish were transferred to a new Petri dish containing fresh artificial fish water and they

were fed with dry food and placed back in the incubator. The water was changed at least one additional time before the experiment.

Immunohistochemistry and confocal imaging

Fish were euthanized and fixed in cooled 4% PFA in 0.25% PBTx (0,25% Triton X-100 in 1X PBS) over night (O/N) at 4°C. Samples were permeabilized in 0.50% Trypsin-EDTA on ice for 40min, then washed. Subsequently the samples were incubated in the blocking solution (2% Normal Goat Serum, 1% BSA, 1% DMSO in 0.25% PBTx) for 1 hour followed by a minimum of 3 hours of incubation in staining solution (1:1000 DAPI, 1% BSA, 1% DMSO in 0.25% PBTx). Samples were finally washed and placed in glycerol. Samples were then placed on a glass slide coated with 1% low-melting-point agarose (LMP, Fisher Scientific), covered with 80% glycerol and a coverslip. Anatomical Z-scans were acquired using a Zeiss Examiner Z1 confocal microscope with a 20x air objective (Zeiss, NA 0.8) at room temperature, using 4-10x average for each plane (Figures 4A and 4B; Figure S5A). For live imaging, prior to embedding, juvenile fish were anaesthetized with 0.02% MS222. Animals were then embedded in 2% low-melting-point agarose (LMP, Fisher Scientific) in a recording chamber (Fluorodish, World Precision Instruments) with AFW. Anatomical Z-scans were acquired using a Zeiss Examiner Z1 confocal microscope with a 20x water-immersion objective (Zeiss, NA 1.0, Plan-Apochromat) at room temperature, using 4-10x average for each plane. In the case of adult zebrafish, the animal was euthanized by immersion in ice-cold water, then decapitated to ensure death. The head was transferred in cold artificial cerebrospinal fluid (ACSF) (Kermen et al., 2020b) bubbled with carbogen (95% O_2/5% CO_2). The eyes, jaws and ventral part of the skull were carefully removed using forceps, exposing the habenula. The brain explant was then affixed using tungsten pins to a small Petri dish coated with Sylgard (World Precision Instruments) and perfused in constant flow bubbled ACSF. Anatomical Z-scans were acquired using a Zeiss Examiner Z1 confocal microscope with a 20x water-immersion objective (Zeiss, NA 1.0, Plan-Apochromat) at room temperature, using 4-10x average for each plane.

QUANTIFICATION AND STATISTICAL ANALYSIS

To perform all the behavioral analysis shown in this study, we used custom-made scripts written in MATLAB.

The heat-maps are an average of zebrafish swimming position over the entire length of each session. For all further analysis, of the baseline session only the last 30 minutes are taken into consideration. We divided each behavioral session into 2-minute time bins to be able to better detect changes over time.

The learning index is defined as follows

$$\frac{(\%\ time\ in\ "conditioning\ zone"\ during\ baseline\ -\ \%\ time\ in\ "conditioning\ zone"\ in\ session\ analysed)}{(\%\ time\ in\ "conditioning\ zone"\ during\ baseline)}$$

To discriminate between learners and non-learners, a lowest boundary for the learning index was calculated, by using the relatively random distribution of zebrafish swimming position during the baseline session. For each animal three control learning indices were calculated over the 1 hour baseline, during each 30 minutes between 0 to 30, 15 to 45 and 30 to 60 minutes. Of the obtained distribution of control learning indices during baseline, the mean+std was used to determine the threshold discriminating learners and non-learners. All fish that exceeded this lowest boundary were considered to exhibit significant learning upon CPA training.

For quantifying swimming direction and avoidance behaviors, the position was detected when fish were near the midline boundary between conditioned zone and safe zone. Next, the linearized trajectory of the animal in the five seconds following the encounter with the midline boundary was used as approach and avoidance, respectively. We then quantify, in 5-minute time bins, the successful avoidance rate of the animals. If the position of the animals was in the ''conditioned zone'' after they encountered the midline the avoidance was considered unsuccessful, otherwise it was considered successful. To calculate avoidance, we iterated multiple distances away from the SZ/CZ boundary (Figure S3), which did not affect our conclusions. The same 5 minutes time bins were used to calculate, swim duration up on each entry to CZ and swim distance up on each entry to CZ and number of entries to CZ.

In reversal learning experiments, we only continued the reversal protocol with those animals that exhibited prominent CPA learning in the first training session and classified as learners using our learning index criterion. If animals did not learn the initial CPA task, they were not subjected to reversal learning.

Choice of statistical analysis

The Wilcoxon rank sum test (ranksum function in MATLAB) was used to quantify statistical differences between two different populations of fish. The data points in all time-bins were pooled together within each session for each experimental group. The statistical test was then performed between the obtained distributions and compared across experimental groups. When comparing intra-group measurement over the course of the protocol, the entire baseline period was used in order to have a robust estimate of baseline behavior on a population level. Then, each time bin was compared to this baseline distribution. The Wilcoxon signed-rank test (signrank function in MATLAB) was performed when individual behavior was compared between two different conditions. Detailed information about the statistical test performed and p values can be found in each figure legend.